

*This paper has considered improving the management of energy consumption by a photovoltaic system with a storage device for a local object connected to the network. The aim of the study is to reduce expenditures when paying for electricity consumed from the network, when loading an object, independent of the time of year, and to eliminate energy generation to the grid. An energy generation control algorithm has been improved whereby the state of battery charge during the day is based on a forecast. That could reduce electricity consumption at night with better utilization of rechargeable battery and photovoltaic battery power during the day. It is proposed to use autonomous operation by disconnecting from the network during peak tariff hours and during the day with enough energy generation by a photovoltaic battery. This would ensure the normal functioning of an object in the event of a possible deterioration in the quality of voltage in the network while reducing the loss of energy in the inverter. Predictive control of the expected battery charge at the next checkpoint (at 0.5 hours or less between control points) has been proposed. A control system structure has been developed whereby a rechargeable battery current is set depending on an operational mode, the tariff zone, and the projected generation by a photovoltaic battery while reducing the modulation frequency under an autonomous mode. In this case, the modes are switched and the structure is changed taking into consideration the state of battery charge. Simulation in the daily cycle has shown the possibility of reducing the cost of electricity consumed from the network by 1.7–8 times at two or three tariff rates. Simulation of electromagnetic processes in the system confirms acceptable regulation indicators when switching the structure, as well as a decrease in the energy loss in an inverter under an autonomous mode by up to 40 %*

**Keywords:** energy redistribution, rechargeable battery charge state, control structure, predictive control, autonomous mode, battery current regulation, multi-zone pricing

UDC 620.91:621.31

DOI: 10.15587/1729-4061.2021.228941

# IMPROVED CONTROL OF ENERGY CONSUMPTION BY A PHOTOVOLTAIC SYSTEM EQUIPPED WITH A STORAGE DEVICE TO MEET THE NEEDS OF A LOCAL FACILITY

**Olexander Shavolkin**

Doctor of Technical Sciences, Professor\*

E-mail: shavolkin@gmail.com

**Iryna Shvedchykova**

Doctor of Technical Sciences, Professor\*

E-mail: shvedchykova.io@knu.edu.ua

**Jasim Mohmed Jasim Jasim**

PhD, Associate Professor

Department of Electrical Power Engineering Techniques

Al-Furat Al-Awsat Technical University –

Al-Musssaib Technical College

Al-Najaf Baghdad main road, 15, Al-Kufa, Iraq, 54001

\* Department of Computer Engineering and Electromechanics

Kyiv National University of Technologies and Design

Nemyrovycha-Danchenka str., 2, Kyiv, Ukraine, 01011

Received date 26.02.2021

Accepted date 01.04.2021

Published date 30.04.2021

**How to Cite:** Shavolkin, O., Shvedchykova, I., Jasim, J. M. J. (2021). Improved control of energy consumption by a photovoltaic system equipped with a storage device to meet the needs of a local facility. *Eastern-European Journal of Enterprise Technologies*, 2 (8 (110)), 6–15. doi: <https://doi.org/10.15587/1729-4061.2021.228941>

## 1. Introduction

As the share of green energy, including small (local facilities (LFs) with renewable sources), increases, there is an increasing number of issues related to ensuring the balance of energy both in the energy system in general and in local microgrids. This is primarily due to the mismatch between generation peaks and the peaks of consumption. That has led to new development trends and approaches to system design, including a reduction in green tariffs [1]. An effective, but expensive, solution is the use of storage devices. Also rational is the approach to using energy where it is generated, when LF (a small business object, cottage) takes on the role of the prosumer in the energy market system [2, 3]. The ability to shift consumption from peak hours to less active night and day periods, when there is a storage battery (SB) in the photovoltaic system (PVS), contributes to ensuring the balance of energy in the grid. However, the use of SB in PVS leads to an increase in the cost of the system, so the return on investment, along with the improved reliability of

the electricity supply, is achieved by reducing costs. Thus, it is a relevant task to improve the management of energy consumption by PVS with a storage device in order to meet the LF needs while reducing the cost of electricity consumed from a distribution grid (DG).

## 2. Literature review and problem statement

Actual PVSs with SBs widely employ hybrid inverters, which contain the entire set of equipment for connecting a photovoltaic battery (PV) and SB with the appropriate software. Hybrid inverters are produced by many manufacturers, such as ABB [4], Conext [5], with a capacity of up to 10 kVA and the possibility of combining three single-phase ones into a three-phase system of 3\*10 kVA. Hybrid inverters are designed to reduce the consumption of electricity from DG. At the same time, when PV's energy is not enough to provide load, the SB energy is added to it. There are functions of charging from the network, operation under an au-

tonomous mode (AM) when disconnected from the network. They have ample control capabilities that enable the setting of operational priorities (from the network, the Sun, SB) and control over the Internet. They are intended to use a single tariff rate and do not have the function of redistribution of energy during the day.

Promising for use in LF PVS are the multifunctional inverters that generate surplus electricity in DG while providing for a power factor close to unity at the point of connection to the network. A variant of PVS with non-linear load is considered in [6]; the unbalanced load for phases is taken into consideration in [7]. However, the application of SB in PVS is not considered.

Paper [8] reports PVS with SB and four DC converters with a common link: the PV voltage level; two bidirectional converters of DC into DC for SB and a supercapacitor; a grid inverter. The selection of the maximum power of PV is provided by the MPPT controller. The power storage control channel uses a proportional-integral (PI) voltage controller in a DC link. The controller sets the battery and supercapacitor current. A “multiconverter” provides for the predefined active power with the proper quality of electricity; PV’s operation with tracking the maximum power point; extending battery life through a hybrid storage system. However, its use is seen as a distributed energy unit in a collective system run by a centralized smart energy management system.

A similar structure, but without a supercapacitor for PVS with SB, is described in [9]. This resolves the issue of combining several PVSs into an autonomous system when the network is disconnected. The task of managing energy consumption is not considered.

The algorithm of energy dispatching in a networked PVS with a rechargeable storage system is considered in [10]. The aim is to determine the most appropriate (optimal) hours for switching between SB, PV, and DG, based on data on the history of consumption by LF. The optimal amount of energy accumulation is also determined, which is introduced during peak demand. This provides for the generation of excess energy in DG; SB is charged from PV during daylight time (no charge of SB from the network is used). PV and SB connect to the grid inverter through the keys; control is reduced to managing those keys. To assess the effectiveness, the authors performed a simulation in the daily cycle, however, at the level of the declaration; they described only a simplified model of the inverter.

Great importance in improving the efficiency of PVS is given to forecasting the generation of PV, which makes it possible to plan the load, to use different scenarios of PVS operation. The use of neural networks looks promising [11]. However, a variety of web services, such as [12], have recently been presented for a wide range of PB generation forecasting capabilities. Work [13] reports an open web service that gives consumers access to individual projections of their future solar energy generation according to weather conditions for their location.

In [14], models are proposed for predicting the power of PV with a resolution of 5 minutes using weather variables with a resolution of 1 hour, which improves the accuracy of the forecast.

In [15], an energy consumption control system is presented for an autonomous microgrid with PVS and SB without connecting to DG. A predictive approach is used to set work schedules. At the same time, the online weather forecast, updated four times a day, combined with the model

of the photovoltaic system makes it possible to predict energy generation within 48 hours. These forecasts are used alongside load forecasts and an energy storage system model to predict the rechargeable battery charge state. The goal is to minimize downtime in the microgrid, in particular by the pre-emptive discharge of the load.

The simulation of a hybrid energy storage system for solar microgrid systems connected to the network of residential buildings in the daily cycle is considered in [16]. The dynamic models of SB and a supercapacitor are represented in MATLAB (USA); the smoothing of load fluctuations is explored. There is no research on energy management and redistribution in the system.

The issue of ensuring the efficient operation of PVS with SB for LF, when the power consumed by the load does not depend on weather conditions, needs further consideration. Note that the load scenario is likely the same; there is an opportunity, considering the forecast, to increase the load if necessary. At the same time, the possibility of accounting for the weather forecast to improve control over the SB charge-discharge is not used. With the exclusion of excess energy generation in DG, the system has three regulated parameters: the power generation capacity of PV, the power (current) consumed from the network, the state of SB charge. At different intervals, the implementation of the work is different. Thus, in the half-peak morning hours, SB charging is impractical, during the hours of significant generation by PV the charge current depends on the power of generation. With a small generation by PV, the task is to provide the maximum charge of SB; at night, one should charge SB to a certain (sufficient) value.

In the absence of consumption from DG, one should consider switching to an autonomous mode of operation, which gives a positive effect – eliminating the impact of network voltage quality breach on LF consumers. Switching is desirable to carry out discreetly for the consumer – without pauses.

The hours of the tariff zones change by the seasons of the year, and the distribution of highs in the load schedule of LF may change. A convenient tool for assessing the effectiveness of PVS management is the simulation of energy processes in the daily cycle of operation, which implies the existence of a correct model without taking into consideration transitional processes and harmonics. The study of electromagnetic processes in the system and the assessment of energy losses in the keys suggests the presence of a detailed model.

---

### 3. The aim and objectives of the study

---

The aim of this work is to improve control over energy consumption by PVS with SB to meet the needs of LF connected to the network, to reduce the cost of electricity at a load that does not depend on the time of year while eliminating energy generation to the network.

To accomplish the aim, the following tasks have been set:

- to improve the mechanism that manages the generation and redistribution of energy in PVS using predictive control;
- to develop a PVS control system;
- to perform simulations that estimate lower payment costs when using different tariff plans;
- to develop a detailed model of the system “DG – PVS with SB – load” to study the automatic control system performance and assess energy losses in the inverter.

**4. Materials and methods to study the improved control over energy consumption by a rechargeable battery-powered photovoltaic system**

We studied ways to improve the mechanism of control over energy generation and redistribution in PVS based on methods of analysis of electrical circuits. The analysis of energy processes was performed in the daily cycle disregarding transitional processes and higher harmonics in energy converters. Energy losses were accounted for through efficiency ratios. The manufacturer’s specifications were taken into consideration for SB. The generation of PV was set on the basis of archival data. The implementation of predictive control took into consideration possible deviations of the PV power forecast from the actual (measured data) value at control points. The predicted values of the state of charge were determined taking into account the measured values. In determining the thresholds of SB charge, at switching, the SB charging characteristics at a depth of discharge (DOD) of 50 % were used. The control system is implemented on the basis of a classic two-contour structure. The parameters for the network inverter output filter have been justified, according to our calculations, based on the amplitude-frequency characteristic considering the network resistance. Electronics Workbench (Canada) software was used for this purpose. The simulation was performed using the verified MATLAB (USA) software package. The simulation model of energy processes is based on estimation expressions, taking into consideration changes in the structure of the control system and SB characteristics. A detailed model of electromagnetic processes in the system employs standard functions and blocks from the MATLAB library (USA). The loss in transistors was estimated at instantaneous current values based on transistors data and Semikron recommendations.

**5. The results of a study to improve the principles of energy control and redistribution in a photovoltaic system with rechargeable batteries**

**5.1. Improving the mechanism for managing the generation and redistribution of energy in a photovoltaic system using predictive control**

The structure of PVS with SB, using an example of a single-phase implementation variant (Fig.1), includes a grid inverter (VSI) with an output LCR filter [17, 18], a photovoltaic battery (PV) and a rechargeable battery (SB), LF load, distribution grid (DG). PV connects to the VSI input via the DC/DC1 booster; SB – via DC/DC2 (charge controller) with two-way conductivity. The LF load is connected to the VSI output and, through contactor K with a VS triac, to DG. Contactor K is needed to disconnect PVS from DG in the absence of voltage (an emergency mode). VS is used to avoid a pause when one connects to DG when the voltage is restored (K1 is first closed, and, after the VSI  $u_C$  voltage is synchronized with the network voltage  $u_g$ , the

triac is activated). To measure the short-circuit current PV, the QS switch is used [18]. Voltage and current sensors are not shown in Fig. 1.

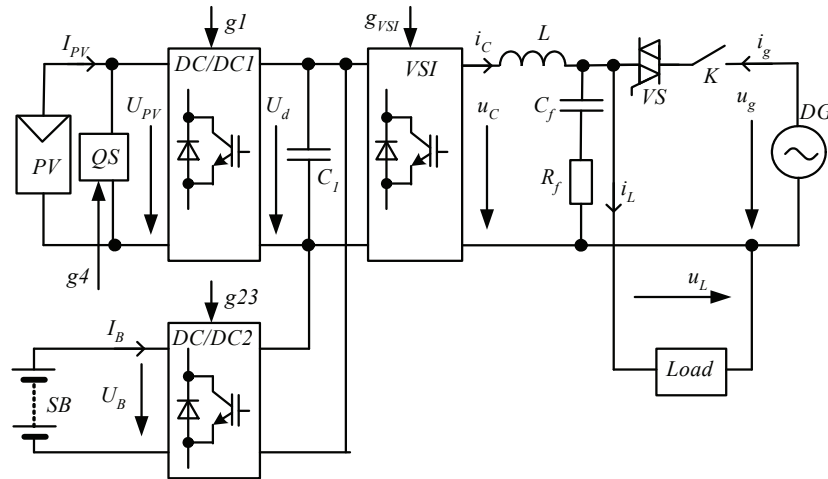


Fig. 1. The structure of PVS power circuits

A three-zone tariff at peak loads during the morning and evening hours is traditional for most countries [3, 19]. Temporal zones are somewhat shifted for different seasons.

In this case, for example, in accordance with [19], there is the following alternation of zones and cost ratios:

- $(t_1-t_2)$  – half-peak (daytime)  $d$  with a coefficient  $T_d=1$ ;
- $(t_2-t_3)$  – peak  $m$  with  $T_p=1.5$ ;
- $(t_3-t_4)$  – half-peak  $d$  with a coefficient  $T_d=1$ ;
- $(t_4-t_5)$  – peak  $e$  with a coefficient  $T_p=1.5$ ;
- $(t_5-t_6)$  – half-peak  $d$  with  $T_d=1$ ;
- $(t_6-t_1)$  – night  $n$  with a coefficient  $T_n=0.4$ .

SB has two discharge cycles per day. For lead-acid SBs, the acceptable value of DOD does not exceed 30–50 %. For example, for OPzV12-100 RB, the number of discharge cycles is about 3,000 at DOD=50 % [20]. Lithium SBs demonstrate the best performance but they are a little more expensive. Thus, DOD needs to be monitored and limited (DOD≤50 %). It is also necessary to consider that at an SB charge state of  $Q^*=100 \cdot Q/Q_R \geq 80\%$  ( $Q$  and  $Q_R$  are the actual and rated values, respectively) the  $I_B$  current is significantly reduced and, accordingly, the ability of the SB to receive energy is significantly reduced.

Taking into consideration losses in the converter ( $\eta_C$  is the efficiency of the converter) and in SB ( $\eta_B$  is the SB efficiency), the energy transferred to the load, for PV and SB

$$W_{PVL}=W_{PV} \cdot \eta_C, W_{BL}=W_B \cdot \eta_B \cdot \eta_C,$$

where  $W_B=U_B C_B$  is the SB energy intensity (W·h);  $C_B$  is the capacity (A·hour).

We set a task to, while ensuring the constant load of LF during the year, to eliminate (in winter, reduce) electricity consumption from the network during peak hours  $P_g=0$ . At the same time, regardless of the  $P_{PV}$  power generated by PV, and the load capacity  $P_L$ , the PVS operates under an autonomous mode AM, using the PV energy  $W_{PV}$  and SB energy  $W_B$ .

During the evening peak, the PB’s PV’s energy is low and, accordingly, the SB capacity determines the allowable LF load capacity  $P_{LA5}$ , taking into consideration the state of discharge  $\Delta Q_{45}^*=Q_{45}^*-Q_{41}^*$  (assume  $Q_{45}^* \geq 50\%$ ,  $Q_{41}^* \geq 85\%$ )

$$P_{L45} = \frac{\Delta Q_{45}^* W_{BL}}{(t_3 - t_4)}. \quad (1)$$

During the morning peak ( $t_2, t_3$ ),  $W_{PV23} > 0$ , which makes it possible to increase  $P_{L23} > P_{L45}$  if necessary. Accordingly, for  $t_2$ , one needs to have a certain (sufficient) value  $Q_2^*$ . With an increase in the PV generation (spring – fall – summer) there is a growth in  $W_{PV23}$ , and there is no sense to provide for the maximum value  $Q_2^*$  by the beginning of the morning peak. This reduces energy consumption to charge SB; more complete use of PV energy in the hours of maximum solar generation is achieved. The value of  $Q_2^*$  can be determined according to  $W_{PV23}$  based on the weather forecast for the following day. The night charging of SB stops after reaching the predefined value of  $Q_2^*$ . After a partial discharge during peak hours, SB should have time to charge from PV in the daytime hours to the value of  $Q_d^* > 90\%$ , maximizing the PV energy utilization. In accordance with the generation by PV, for a clear day, it is possible to accept  $t_d = 16.00 - 16.30$  as a checkpoint for the spring–summer–fall period, when it is still possible to meet the condition  $P_{PV}\eta_C > P_L$  and it is possible to additionally charge the SB. In winter, the daily charging of SB is generally unrealistic. We believe that in the interval ( $t_3, t_d$ ) the average value is  $P_{L3d} = P_{L45}$ , then

$$Q_2^* = Q_d^* - \frac{100}{W_B} \left[ \frac{W_{PV3d}\eta_C\eta_B - P_{L3d}(t_d - t_3)\eta_B}{+ \frac{W_{PV23}\eta_C}{\eta_B} - \frac{P_{L23}(t_3 - t_2)}{\eta_B}} \right]. \quad (2)$$

General recommendations include the expediency of reducing  $P_L$  in the evening ( $t > t_d$ ), when  $W_{PV}$  falls significantly even on a clear day. During peak hours, when DG is overloaded, there may be an unacceptable deviation of the network voltage from the rated one. That is possible during other hours as well. Under an autonomous mode, when PVS is disconnected from the network, the load voltage  $u_L$  is set based on the rated value  $u_{LR}$  accompanied by the corresponding recalculation of  $P_L^1$ . Under an emergency autonomous mode (no DG voltage), the voltage  $u_L$  may decrease to maintain the charging of SB [21].

After the morning peak, the mode of operation is determined by the ratio of  $P_{PV}\eta_C$  to  $P_L$ . If  $P_{PV}\eta_C > P_L^1$  ( $P_L^1$  is the measured load power recalculated for  $u_{LR}$ ), the AM1 mode (Table 1) is used.

If  $P_{PV}\eta_C < P_L^1$ , the system is switched to work in parallel with the GM network. However, this would lead to consumption from the network, which is not always advisable. For example, if the difference  $\Delta P = (P_{PV}\eta_C - P_L^1)$  is insignificant, and the time interval when it occurs is short, it would not result in a large decrease in  $Q^*$ . That is the condition  $\Delta P < 0$  is not sufficient and information is needed on where this could lead. Let us consider a predictive solution involving determining the value of  $Q^*$  the value one step ahead using the data on PV generation forecast  $P_{PVP}(t)$ . At the same time, the daytime period of PVS operation is split into a series of checkpoints at intervals  $\Delta t = 0.5$  hours or less (considering the possibility of changing the load, the accuracy increases with the reduction in the duration of the interval). The dependence  $P_{PVP}(t)$  is recalculated to the value of  $P_{PVAVP}(t)$ , averaged over the interval. At the current  $i$ -th checkpoint, the actual values of  $Q^*$ ,  $P_{PVfi}$ ,  $P_{Li}$ ,  $P_{PVAVPi}$  are known (average PV power and loads at intervals of a few minutes are used). The actual

value of  $P_{PVfi}$  may differ from the forecast value  $P_{PVPi}$ . Given this, the value is recalculated

$$P_{PVAVPi} = \frac{P_{PVfi}}{P_{PVPi}} P_{PVAVPi}.$$

We believe that the load in the interval to the next point ( $i+1$ ) is constant, then the increment

$$\Delta Q_i^* = 50 \frac{P_{Li} - P_{PVAVPi}}{W_{Bf}}$$

and the predicted value  $Q_{i+1}^* = Q_i^* + \Delta Q_i^*$  (if  $\Delta Q_i^* < 0$  and  $\Delta Q_i^* = 0$  if  $\Delta Q_i^* > 0$ ). If the value  $Q_{i+1}^* > Q_R^*$  ( $Q_R^*$  is the predefined value), the system continues to work under an autonomous mode (at close values the  $Q_{i+1}^* \approx Q_R^*$  voltage is reduced to  $0.95 U_R$  and, accordingly, the load capacity by 10%), if not – the system switches to work from the network. The specific value of  $Q_R^*$  is set for each interval. In the evening hours, in the run-up to the evening peak, we proceed from the time of SB charging. In accordance with the charge characteristics of a lead-acid SB [20], it can be taken that at  $Q^* \geq 80\%$  it is possible in 0.5 hours to charge by 3%, at  $Q^* < 80\%$  – charge by 5%. Thus, at  $t_d = 20.00$  at  $t_i = 19.30$   $Q_R^* = 86\%$ , at  $19.00 - Q_R^* = 83\%$ , at  $18.30 - Q_R^* = 80\%$ , at  $18.00 - Q_R^* = 75\%$ . In the interval to  $16.00 - Q_R^* = 85\%$ . Return to the autonomous mode is carried out by the condition  $P_{PV}\eta_C > P_L^1$  or  $Q^* \geq 92\%$  (further charging of SB is significantly slowed down and does not make sense).

## 5.2. The structure of a photovoltaic system control system

The control system (Fig. 2) is two-contoured. It includes an internal circuit of current control (CCL) of the inverter and three proportional-integral (PI) voltage controllers VC, VC2, VC3 to stabilize the voltage at the inverter input  $U_d$  at the predefined level  $U_d^1$  [22, 23]. CCL can be implemented using a relay current controller [22, 23], or width-pulse modulation (PWM). Below we consider an option with PWM. In the absence of generation in DG, LF PVS is a consumer of energy for DG. That makes it possible to slightly reduce the requirements for the quality of the output current in the inverter, which consumes current from the network only if the PV energy is not enough to charge SB, and in the process of night charging.

In the presence of an external voltage controller, which sets the current amplitude of the inverter  $I_{Cm}$ , the structure of the current control contour would do with a proportional link with the coefficient

$$k \leq \frac{1}{4\Delta I_{CmMAX}}$$

without compensating for a static error caused by the perturbing effect  $u_g$  [17]. To reduce energy loss to switch the inverter transistors under an autonomous mode, the  $f_M$  value can be reduced by recalculating the value of  $k$ . We assume the power of the inverter to be 5.5 kVA at the maximum value of the output current  $I_{CmMAX} = 25$  A ( $I_{CmMAX} = 35.35$  A). We believe that  $W_B = 15$  kWh and, at  $I_B = 0.1 C_B$ , the power consumed by RB charging would equal  $P_B = 1.5$  kW. The current consumed by the inverter from the network is  $I_C = 6.81$  A (the amplitude is  $I_{Cm} = 9.64$  A). The maximum value of the amplitude of inverter current pulsations is

$$\Delta I_{CmMAX} = \frac{aU_{gm}}{16Lf_M},$$

where  $a>1$ ,  $U_{gm}$  is the amplitude of DG voltage,

$$L = \frac{bU_{gm}}{\omega I_{CmMAX}}$$

is the inductivity of the inverter output filter reactor,  $I_{CmMAX}$  is the amplitude for the maximum value of the inverter current  $I_{CMAX}$ ,

$$b = \frac{U_L}{U_g} = \frac{\omega L \cdot I_{CMAX}}{U_g}$$

is the reactor voltage value (first harmonic) for  $I_{CmMAX}$ , relative to the voltage of DG;  $\omega$  is the angular frequency of network voltage.

Assume

$$a=1.15 (U_d=aU_{gm}=360 \text{ V}), b=0.0375 (L=0.00105 \text{ H}).$$

At the frequency of modulation of  $f_M=6.8 \text{ kHz}$ , we obtain  $\Delta I_{CmMAX}=3.12 \text{ A}$ . Taking into consideration the value of  $I_{Cm}=9.64 \text{ A}$ , we accept that, in order to ensure an acceptable harmonic composition of the current  $I_C$ , the output filter of the inverter for  $f_M$  should enable suppression on the order of about 10 times ( $G=-20 \text{ dB}$ ). This is confirmed by the analysis of the frequency response of the filter in the EWB program under the following parameters: for the reactor,  $L=0.00105 \text{ H}$ ,  $R=0.1 \text{ Ohm}$ ;  $C_f=60 \text{ }\mu\text{F}$ ,  $R_f=0.3 \text{ Ohm}$ . In this case, the network resistance is  $R_C=0.02 \text{ Ohm}$ ,  $X_{LC}=0.02-0.04 \text{ Ohm}$ .

VC, VC1 controllers with a S1 switch (position 1 at GM, position 2 under AM and AM1 modes (Table 1)) enable control over the inverter. VC2, VC3 controllers enable, respectively, the regulation of PB generation and RB charge. The PB regulation channel also includes a MPPT controller; a measurement unit (MU) of PB short-circuit  $I_{SC}$  (enables periodic closure of the key QS). The S2 switch sets the mode – position 1 when setting the PV current from MPPT, position

2 – from VC2. The limitation unit (LU) sets the PV current value  $I_{PV}^1$  at the level of  $I_M=(0.92-0.95)I_{SC}$ , close to the maximum power mode. The DC/DC1 control system ( $CSC_{PV}$ ) is executed with an  $I_{PV}$  current relay. In this case, control over PV generation [18] is carried out by the MPPT controller or VC2 (Table 1). VC2 maintains the energy balance in the system by adjusting  $I_{PV}$  and  $P_{PV}$  in accordance with energy consumption by the load and SB. Thus, under AM mode, the MPPT controller enables the selection of the PV maximum power. Under AM1 mode, the SB charge current task is set

$$I_B = \frac{P_{PV}\eta_C - P_L^1}{U_B}. \tag{3}$$

The actual value of  $I_B$  is limited to the allowable value  $I_B=I_{BRMAX}$  ( $I_{BR}=(0.1-0.2)Q_R$ ) and is determined by the value of  $Q^*$ . VC2 operates until the cut-off at  $I_{PV}=I_M$ , and, when RB cannot accept the difference in the PB and load power, VC2 reduces the generation by PB.

The SB current control channel includes: VC3; a CCU charge controller, which determines  $Q^*$ , switches the setting of  $I_B$  (from VC3 or CU), and sets a current limit; a DC/DC2 ( $CSC_{SB}$ ) control system.

Under an emergency autonomous mode, when voltage is turned off in DG, AM1 is used to adjust the power of PV.

The PLL phase adjustment unit forms the function  $\sin\omega t$  based on the network voltage  $u_g$ , and, under AM mode, it operates as a standalone generator with a frequency of 50 Hz. A  $u_S$  synchronization signal is also formed when switching from AM (AM1) to GM.

The switch control functions in the structure are performed by the CU control unit, depending on the ratio of  $P_{PV}$  to  $P_L$  (Table 1), the current measured and projected value of  $Q^*$ , the signals from sensors and the energy control system signals from an external software control device (SCD).

The input data for SCD are the data on PVS installation: the power of PV and SB, tariff zones, broadcast data of the forecasted PV generation from a weather website. In this case, the measurements can determine energy consumption, estimate the reduced payment.

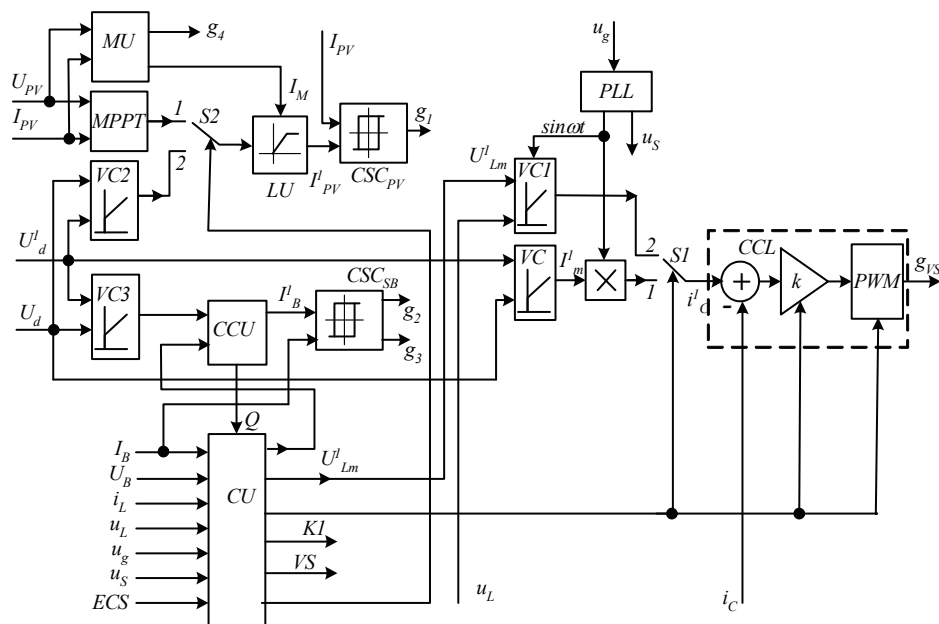


Fig. 2. Control system structure

Table 1

Daily cycle operational modes				
$(t_1-t_2), (t-t_6)$	$(t_2-t_3), (t_4-t_5)$	$(t_3-t_4)$		$(t_6-t_1)$
GM	AM	AM1	GM	GM
$gm=1$	$am=1$	$am1=1$	$gm=1$	$gm=1$
$P_{PV}=P_{PVP}$ $P_B=0$	$P_{PV}=P_{PVP}$ $P_B = I_B^1 \cdot U_B$	$P_{PV} = P_L^1 + P_B$ $P_B = I_B^1 \cdot U_B$	$P_{PV}=P_{PVP}$ $P_B = I_B^1 \cdot U_B$	$P_{PV}=P_{PVP}$ $P_B = I_B^1 \cdot U_B$
$Q_s^* = Q^*$	$Q^* > 50\%$	$P_{PV} \eta_C > P_L^1$	$P_{PV} \eta_C < P_L^1$	$Q_s^* \geq Q^* > 50\%$
$I_B=0$	$I_B = (P_{PV} \eta_C - P_L^1) / U_B$	$I_B = (P_{PV} \eta_C - P_L^1) / U_B$	$I_B = I_{BRMAX}$	$I_B = I_{BR}$
$P_g = P_L$	$P_g = 0$	$P_g = 0$	$P_g = P_L - P_{PV} \eta_C + P_B / \eta_C$	$P_g = P_L + P_B / \eta_C$
MPPT, VC	MPPT, VC1, VC3	VC1, VC2	MPPT, VC	MPPT, VC

**5. 3. Simulation model of energy processes in a photovoltaic system**

This model implements the daily cycle of PVS operation; transition processes are not taken into consideration; energy losses are taken into consideration through efficiency.

The model includes: a PV generation module, an SB model, an LF load (set in a tabular form), a mode job module, a calculation module, a cost assessment module.

The generation module forms  $P_{PVP}(t), P_{PVAVP}(t), P_{PVf}(t)$  in accordance with the forecast (we use archival data from [24], when reducing the generation by PV (AM1 mode) – in accordance with  $P_L$  and  $P_B$  (Table 1). To measure  $P_{PVP}, P_{PVf}$  values at checkpoints, a sampling-storage device is used. The mode job module forms variables corresponding to the tariff zones  $d, m, p, n$ , as well as variables that correspond to  $gm, am, am1$  operational modes.

The SB model is based on data from catalogs. Taking into consideration energy loss, the SB charge is

$$Q = Q_s + \int I_B^1 dt,$$

where  $I_B^1 = I_B \eta_B$  – when charging SB, and  $I_B^1 = I_B / \eta_B$  – when discharging SB.

In this case, the  $I_B$  value is formed as  $I_B(Q^*)$ , in accordance with SB specifications [20]. The  $I_{Brcmax}$  restriction has been introduced at discharge. The adjustable limit is used: the upper limit is set by  $I_B(Q^*)$ , and the lower limit – by  $I_{Brcmax}$ . The SB voltage is also set in the form of the dependence  $U_B(Q^*)$ . A storage sampling device is used to measure the values of  $Q^*$  at checkpoints.

Based on Table 1, GM calculates  $I_B, P_B$ , the power  $P_g$  consumed from DG. To estimate the reduction in the cost of electricity consumed from the grid, the cost-assessment module uses the coefficient  $k_E = C_1 / C_2$  ( $C_1$  is the cost of electricity consumed by LF load,  $C_2$  is the cost of electricity consumed from DG). Accordingly

$$k_E = \frac{W_{Ld} T_d + W_{Lm} T_m + W_{Le} T_e + W_{Ln} T_n}{W_{gd} T_d + W_{gn} T_n},$$

where  $W_{Ld} = \int P_L \cdot (gm \cdot \bar{n}) dt$  is the energy consumed in the intervals consistent with GM's daytime regime; similarly determined are  $W_{Lm}, W_{Le}, W_{Ln}$  for AM (variable  $am$ ), AM1 (variable  $am1$ ), and, at night (variable  $n$ );  $W_{gd} = \int P_g (gm \cdot \bar{n}) dt$ ,  $W_{gn} = \int P_g ndt$  is the energy consumed from DG during the daytime and night periods, respectively.

**5. 4. MATLAB simulation results**

The simulation was performed for PV ( $P_{PVR}=1$  kW) using data from [24] for Kyiv (Ukraine).  $W_B=3,000$  W·h at  $\eta_B=\eta_C=0.94$  and  $W_{Bf}=2,651$  W·h. On a clear day in June 2015, the total daily PV generation was  $W_{PVCs} \approx (6-6.1)$  kW·h. Assume that the evening peak tariff zone [19] is 3 hours (20.00–23.00), then, in accordance with (1),  $P_L = P_{L45} = 309$  W (taken as 300 W). The system performance is considered under a load independent on the PV generation (Table 2). In this case, in the evening peak in winter, the exclusion of consumption from PV is ensured only from 17.00 to 20.48.

Table 2

Load schedule						
Summer						
$t, h$	7.00–8.00, 23.00–24.00	8.00– 11.00	11.00– 16.00	16.00– 20.00	20.00– 23.00	24.00– 7.00
Winter						
$t, h$	6.00–8.00, 21.00–23.00	8.00– 10.00	10.00– 15.00	15.00– 17.00	17.00– 21.00	23.00– 6.00
$P_L, W$	188	413	300	188	300	109

The simulation was carried out on the condition that the actual PV generation is 0.9 of the forecast value. The  $k_E$  values for different pricing plans with load and consumption payment estimates from PV at the same rates are:  $k_{E1}$  (one rate  $T_d=1$ ),  $k_{E2}$  (two rates  $T_n/T_d=0.5/1$ ),  $k_{E3}$  (three rates 0.4/1/1.5); they are given in Table 3. Three July days in 2015 were considered ( $W_{PV}=6, 4.756, 3.367$  kWh) and a clear day in December ( $W_{PV}=1.716$  kWh). In addition, Table 3 gives the  $k_{E21}$  and  $k_{E31}$  values when calculating  $C_1$  for one tariff  $T_d=1$ . The  $Q_2^*$  values were set according to (2). The  $k_{E30}$  values are derived when setting  $Q_2^* \approx 93\%$  regardless of the forecast. In all cases, charging an RB during the morning and night hours with a daily tariff was excluded. For comparison, Table 3 gives the  $k_{E3}^*$  values when control was based on the ratio of  $P_{PV}$  and  $P_L$  power.

Oscillograms of the daily cycle of PVS operation at  $W_{PVP}=4.756$  kWh ( $P_{PVf}$  is the actual value of PV generation,  $P_{PVC}$  is the actual generation considering control) are shown for the following:

- control based on the ratio of  $P_{PV}$  to  $P_L$  power with setting the initial  $Q_2^*$  value (Fig. 3, a). In this case, in the daytime we observe two switches to work from DG ( $k_{E3}=4.07$ );
- control by determining  $Q^*$  one step ahead (Fig. 3, b). At 19.30, at the actual value of  $Q^*=83\%$ , the forecast

value at 20.00 was 80 %, which predetermined switching to the grid operation and RB recharging to 86 %, which is enough to work out the evening peak ( $k_{E3}=5.61$ );

– control by setting AM mode at the initial value  $Q_2^*=93\%$  (Fig. 3, c). In this case, by increasing the night charging of SB, the energy was enough to exclude the connection to the network, although the indicators were worse ( $k_{E3}=5.17$ ).

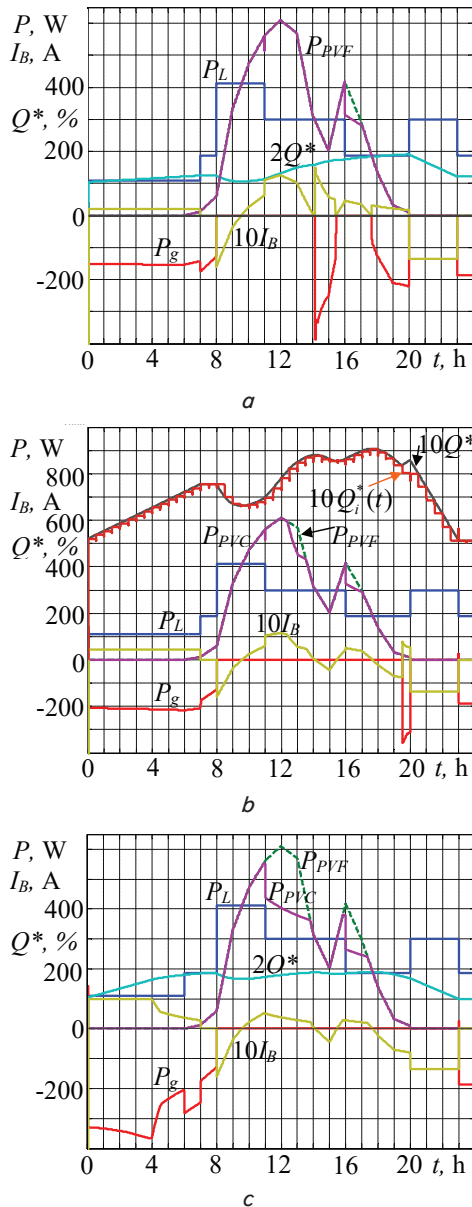


Fig. 3. Oscillograms of the daily cycle of PVS operation at 4.756 kWh under the following control: a – based on the ratio of  $P_{PV}$  to  $P_L$  power and by setting the initial value of  $Q_2^*$ ; b – by determining  $Q^*$  one step ahead; c – by setting AM regime at the initial value  $Q_2^*=93\%$

At  $W_{PVP}=3.367$  kWh (Fig. 4), the decrease of  $Q^*<80\%$  (77 %) was predicted at 13.00, followed by a network connection and charging the RB. At 14.30, at  $Q^*\geq 92\%$ , the system returned to AM with the RB discharge. At 19.00 the next switch to the network is predicted, until 20.00.

The function of adjusting the power of the load by reducing voltage was not used in these cases. This feature is

useful under an emergency autonomous mode when there is no possibility to recharge SB from DG.

Table 3

The values of  $k_E$  for different pricing plans

$W_{PVP}$ , kW·h	$k_{E1}$	$k_{E2}$	$k_{E21}$	$k_{E3}$	$k_{E3}^*$	$k_{E31}$	$k_{E30}$
6	3.7	5.89	6.37	8.19	5.64	7.44	5.69
4.756	2.79	4.14	4.45	5.61	4.07	5.05	4.73
3.367	1.76	2.42	2.6	3.2	2.65	2.89	3.2
1.716	1.36	1.72	1.85	2.165	2.1	1.96	2.165

We also considered PVS operation with an increased SB energy intensity to 4,000 W·h, which yields an effect at high PV generation. For example, at  $W_{PVP}=4.756$  kWh, the value of  $k_{E3}$  is 6.23. However, if  $W_{PVP}$  is reduced, there is no effect; at  $W_{PVP}=3.367$  kWh,  $k_{E3}=3.36$ .

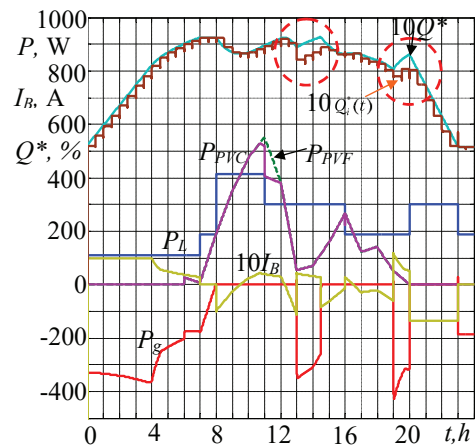


Fig. 4. Oscillograms of the daily cycle of PVS operation at 3.367 kWh

The MATLAB (USA) simulations were also performed by using a detailed model of the system in order to study electromagnetic processes in PVS under the steady and transitional modes. The structure of the model is implemented in accordance with Fig. 1, 2. The model is built according to known principles using a unit to calculate the loss of power in the keys [23] by the instantaneous current and voltage values in accordance with the parameters of the transistors. The model parameters are:  $U_g=220$  V, network resistance  $X_g=0.04$  Ohm, the inverter output filter  $R_f=0.3$  Ohm,  $C_f=60$   $\mu$ F, reactor's  $L=0.00105$  H and  $R=0.1$  Ohm. The capacitor at the inverter output  $C_1=8,000$   $\mu$ F, voltage  $U_d=360$  V. The load is active-inductive. The  $f_M$  frequency for AM is 3 kHz, under a GM mode – 6.8 kHz. When  $f_M$  decreased under AM, the loss of power in the inverter keys decreased to 40 % (the use of IGBT of class 1.2 kV the type of SK 50GH12T4T was considered).

The oscillograms of grid voltage (loads)  $u_g$  ( $u_L$ ), grid current  $i_g$ , inverter current  $i_C$ , current load  $i_L$ , the SB current  $I_B$ , inverter output voltage  $U_d$ , the inverter output voltage  $u_C$  when switching to AM ( $t=0.4$  s) are shown in Fig. 5, a. In this case,  $P_{PV}=0$ , and, up to the moment of switching, the SB was charged from DG through the inverter; after switching, it is discharged, thereby providing the load consumption. Under AM,  $THDu_L=0.87\%$  at  $U_{Lm}=307.8$  V. When connecting the network  $I_{gm(1)}=20.7$  A,  $THDi_g=1.49\%$ . When switching from AM to network operation at  $P_{PV}=1,080$  W (Fig. 5, b), the  $THDu_L$  value is 0.81 % at  $U_{Lm}=308.7$  V; for the current of the network after switching,  $I_{gm(1)}=11.8$  A,  $THDi_g=2.7\%$ .

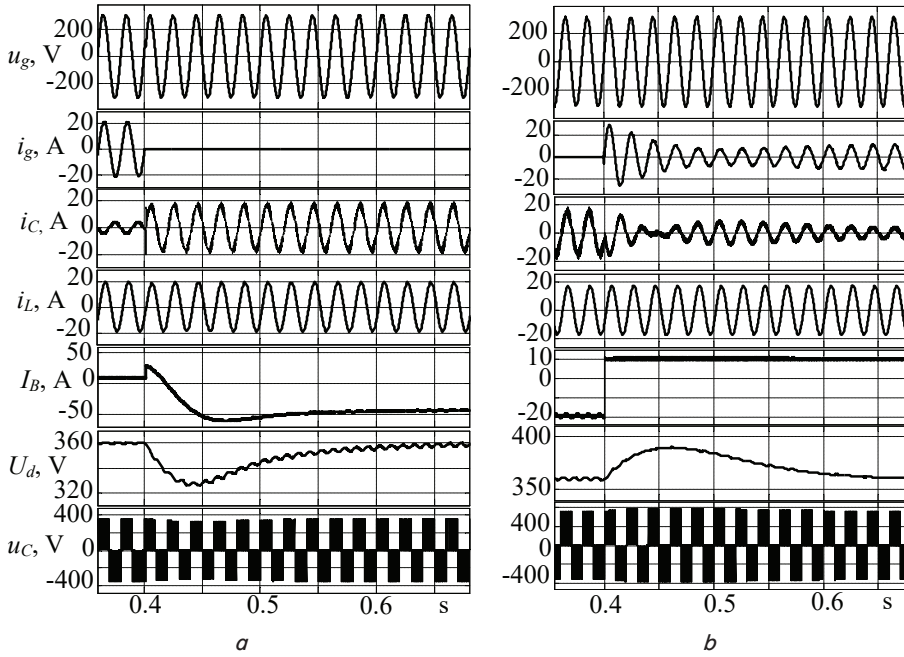


Fig. 5. The  $u_g$  ( $u_L$ ),  $i_g$ ,  $i_c$ ,  $i_L$ ,  $I_B$ ,  $U_d$ ,  $u_C$  oscillograms when switching:  $a$  – from the mode of operation from DG to an autonomous mode;  $b$  – from an autonomous mode to work from DG

In both cases (Fig. 5), the overshoot of voltage stabilization process  $U_d$  does not exceed 10 % with a constant of the filter time in a feedback loop of 0.01 s.

## 6. Discussion of the results of studying the improved control of a photovoltaic system with rechargeable batteries

Improving the mechanism for managing the generation and redistribution of energy in PVS with SB is focused on reducing the consumption of electricity by LF from DG and, accordingly, reducing the amount of payment. Based on the forecasted generation  $P_{PV}(t)$  over the next day, taking into consideration the expected schedule of SB charging, the state of its charge at night is determined according to (2). That eliminates excessive energy consumption at night. Thus, for the case shown in Fig. 3,  $b$ , the sufficient value is  $Q_2^* = 75\%$ , accordingly, the value is  $k_{E3} > k_{E30}$  ( $k_{E30}$  for  $Q_2^* \approx 93\%$ , Table 3). Additional reduction in daily consumption is achieved by using SB energy during the “failures” of PV generation and reduction of generation in the evening hours. In this case, the guaranteed charge of SB to the evening peak is achieved by predicting  $Q^*$  one step ahead (0.5 hours or less) implying the setting of  $Q^*$  thresholds in the appropriate time intervals. The mode switching condition is supplemented by comparing the predicted and the threshold values of  $Q^*$ . Using the PV generation forecast, a possible deviation of the forecast and actual power values of the generation is taken into consideration. A certain reduction in costs due to the cheaper night tariff is achieved by excluding the SB charging in the hours leading up to the morning peak, and after the evening peak with a daily (half-peak) tariff. The transfer of PVS to an autonomous mode disconnecting it from the network in the intervals of time when the energy of PV is enough for the operation of LF contributes to the normal equipment performance.

Based on the condition for ensuring an acceptable harmonic composition of the current of the network inverter when charging SB from the network, the parameters of the output filter and the circuit of the inverter’s current control

have been justified. This provides for a reduction in  $f_M$  under an autonomous mode, which reduces energy loss in the network inverter. In case of DG emergency shutdown, this makes it possible to prolong the time of using the energy of SB in the dark. The control system structure is modified by a control unit in accordance with Table 1. The control unit, along with an external software control device that communicates with the website, implements predictive control functions.

A tool used here to test the proposed principles to control and redistribute energy in PVS, we applied the simulation of energy processes under a daily mode in accordance with Table 1. Predictive control functions have been implemented and the cost of paying for electricity consumed from the grid has been assessed under different tariff plans (Table 3).

The main task in modeling electromagnetic processes in PVS with SB and under a load was to check the feasibility of the system that controls the conversion unit of PVS. The performance at steady and transitional processes during a change in operation was studied; the power loss in the keys of the network inverter was assessed. The acceptable quality indicators of load voltage under an autonomous mode ( $THDu_L \leq 6\%$ , voltage deviation not exceeding 2 %), as well as the current consumed from the grid ( $THDi_g \leq 5\%$ ), have been confirmed. A reduction in the power losses in the transistors of the inverter with a decrease in the modulation frequency under an autonomous mode is up to 40 %. Overshoot in the process of voltage stabilization  $U_d$  does not exceed 10 %.

This work builds on [25] that considered a variant of a standard hybrid inverter at three-zone pricing. In this case, if the energy of PV and SB is enough for the operation of LF load, PVS works under an autonomous mode. When there is not enough energy, the load of LF connects to DG enabling the charging of SB. In the case of excess PV energy, the PV is disconnected while maintaining SB in the active zone, when the  $I_B$  value is limited only to the allowable value. The feature of our solutions is the purposeful formation of  $Q^*$  and a change in the control system using the forecast when taking into consideration the distribution of tariff zones and peak loads.  $P_{PV}$  is adjusted regardless of the control over an SB charge and without limitation on the state of the charge. In the case of switching to an autonomous mode, if the DG voltage deviates unacceptably, the assessment of the ratio of PV capacity and load implies the recalculation to the rated value of voltage. To prevent pauses when switching to an autonomous mode and from an autonomous mode to work in parallel with the network, a triac is introduced in series with the contactor. Switching to an autonomous mode implies changes in the current control and modulation frequency parameters.

There are certain limitations regarding the application of our study results:

– a cycle of LF operation has been considered with the main load during the day and in the presence of peak loads in the morning and evening hours;

– our calculations use a fixed efficiency value  $\eta_C$ , which, in reality, varies within certain limits depending on the load. That also applies to the model.

The study involving the modeling of energy processes in PVS is an estimate of the decrease in energy costs under different tariff plans over a daily cycle. We tested the proposed control implementation principles taking into consideration a change in the current value  $I_B(Q^*)$  relative to the specified value and adjusting the selection of PV power. The study that employed a detailed model mostly focused on implementing the switching modes, assessing control quality, and estimating energy loss in the circuit keys.

To be advanced:

– the implementation of AM emergency regime involving the preparation of recommendations on LF load based on forecasting;

– the study of the principles for enabling energy generation in DG during peak tariff hours, which would make it possible to better utilize the capabilities of RB with enhanced capacity in order to reduce the cost of consumption from DG.

---

## 6. Conclusions

---

1. It is possible to improve the mechanism that controls the generation and redistribution of energy in PVS with SB by using a PB generation forecast. In this case, the reduction in energy consumption at night is achieved by setting the initial state of the SB charge. Reducing the duration of connection to DG during the day is possible by managing the switching of

modes based on the projected charge level, with the differentiation of  $Q^*$  thresholds over the time intervals during 24 hours. With sufficient PB generation, the system functions under AM mode being disconnected from DG, which, when the frequency of modulation is reduced, helps reduce losses in the inverter with the proper voltage quality of LF load.

2. The system of control manages the state of the SB charge based on the forecast of PV generation. There is an adjustment of forecast discrepancies with the actual PV generation. The switching of regimes and changing the control system structure are carried out in accordance with established tariff zones and peak loads. Switching is determined by the predicted charge levels, with the differentiation of thresholds by time intervals. The pauses at mode switching are excluded by using a thyristor, which is enabled sequentially with the contactor when synchronizing the moment of connecting to DG.

3. Our simulation of a daily cycle of PVS operation has shown that the use of SB in the PVS, in order to reduce the cost of electricity consumed from the network, is justified only if there is a tariff rate. The best indicators are achieved at three-zone pricing, producing a reduction in costs from 1.7 to 8 times. Setting the initial SB charge reduces the cost of payment, on a clear day, to 31 %, with a low cloud cover – to 11 %. In general, the proposed predictive control variant makes it possible to increase  $k_{E3}$  by 21 % at  $W_{PVP}=3.367$  kWh (average cloud cover), and by 46 % on a clear day, at  $W_{PVP}=6$  kWh. The solution also applies in the “fair” formation of the hourly payment when the cost of electricity is linked to a load of DG for power.

4. Simulating the electromagnetic processes in the system “DG – PVS with SB – LF load” involving the calculation of losses in the keys of the inverter has confirmed the feasibility of the control system at acceptable indicators under the transitional modes of operation. Reducing modulation frequency under AM decreases power loss in the inverter keys by up to 40 %.

## References

1. Pro vnesennia zmin do deiakykh zakoniv Ukrainy shchodo udoskonalennia umov pidtrymky vyrobnytstva elektrychnoi enerhiyi z alternatyvnykh dzherel enerhiyi. Zakon Ukrainy vid 21 lypnia 2020 r. No. 810-IX. Available at: <https://zakon.rada.gov.ua/laws/show/810-20#Text>
2. Rao, B. H., Selvan, M. P. (2020). Prosumer Participation in a Transactive Energy Marketplace: A Game-Theoretic Approach. 2020 IEEE International Power and Renewable Energy Conference. doi: <https://doi.org/10.1109/iprecon49514.2020.9315274>
3. Nicolson, M., Fell, M., Huebner, G. (2018). Consumer demand for time of use electricity tariffs: A systematized review of the empirical evidence. *Renewable and Sustainable Energy Reviews*, 97, 276–289. doi: <https://doi.org/10.1016/j.rser.2018.08.040>
4. Product manual REACT-3.6/4.6-TL (from 3.6 to 4.6 kW). ABB solar inverters. Available at: [https://seasolargroup.com/wp-content/uploads/2018/08/REACT-3.6\\_4.6-TL-Product-manual-EN-RevBM0000025BG.pdf](https://seasolargroup.com/wp-content/uploads/2018/08/REACT-3.6_4.6-TL-Product-manual-EN-RevBM0000025BG.pdf)
5. Conext SW. Hybrid Inverter. Available at: <https://www.se.com/ww/en/product-range-presentation/61645-conext-sw/>
6. Ma, T.-T. (2012). Power Quality Enhancement in Micro-grids Using Multifunctional DG Inverters. *Proceedings of the International MultiConference of Engineers and Computer Scientists*. Vol. II, IMECS 2012. Hong Kong, 996–1001.
7. Vigneys, T., Kumarappan, N. (2017). Grid interconnection of renewable energy sources using multifunctional grid-interactive converters: A fuzzy logic based approach. *Electric Power Systems Research*, 151, 359–368. doi: <https://doi.org/10.1016/j.epsr.2017.06.010>
8. Guerrero-Martinez, M., Milanes-Montero, M., Barrero-Gonzalez, F., Miñambres-Marcos, V., Romero-Cadaval, E., Gonzalez-Romera, E. (2017). A Smart Power Electronic Multiconverter for the Residential Sector. *Sensors*, 17 (6), 1217. doi: <https://doi.org/10.3390/s17061217>
9. Roncero-Clemente, C., Gonzalez-Romera, E., Barrero-Gonzalez, F., Milanes-Montero, M. I., Romero-Cadaval, E. (2021). Power-Flow-Based Secondary Control for Autonomous Droop-Controlled AC Nanogrids With Peer-to-Peer Energy Trading. *IEEE Access*, 9, 22339–22350. doi: <https://doi.org/10.1109/access.2021.3056451>
10. Slama, F., Radjeai, H., Mouassa, S., Chouder, A. (2021). New algorithm for energy dispatch scheduling of grid-connected solar photovoltaic system with battery storage system. *Electrical Engineering & Electromechanics*, 1, 27–34. doi: <https://doi.org/10.20998/2074-272X.2021.1.05>

11. Mellit, A., Pavan, A. M., Lughi, V. (2021). Deep learning neural networks for short-term photovoltaic power forecasting. *Renewable Energy*, 172, 276–288. doi: <https://doi.org/10.1016/j.renene.2021.02.166>
12. Forecast.Solar. Available at: <https://forecast.solar/>
13. Iyengar, S., Sharma, N., Irwin, D., Shenoy, P., Ramamritham, K. (2014). SolarCast - an open web service for predicting solar power generation in smart homes. *Proceedings of the 1st ACM Conference on Embedded Systems for Energy-Efficient Buildings*. doi: <https://doi.org/10.1145/2674061.2675020>
14. Sangrody, H., Zhou, N., Zhang, Z. (2020). Similarity-Based Models for Day-Ahead Solar PV Generation Forecasting. *IEEE Access*, 8, 104469–104478. doi: <https://doi.org/10.1109/access.2020.2999903>
15. Michaelson, D., Mahmood, H., Jiang, J. (2017). A Predictive Energy Management System Using Pre-Emptive Load Shedding for Islanded Photovoltaic Microgrids. *IEEE Transactions on Industrial Electronics*, 64 (7), 5440–5448. doi: <https://doi.org/10.1109/tie.2017.2677317>
16. Traore, A., Taylor, A., Zohdy, M. A., Peng, F. Z. (2017). Modeling and Simulation of a Hybrid Energy Storage System for Residential Grid-Tied Solar Microgrid Systems. *Journal of Power and Energy Engineering*, 05 (05), 28–39. doi: <https://doi.org/10.4236/jpee.2017.55003>
17. Shavolkin, O., Shvedchikova, I., Kravchenko, O. (2019). Three-phase Grid Inverter for Combined Electric Power System with a Photovoltaic Solar Battery. *2019 IEEE International Conference on Modern Electrical and Energy Systems (MEES)*. doi: <https://doi.org/10.1109/mees.2019.8896661>
18. Shavolkin, O., Shvedchikova, I. (2020). Improvement of the Three-Phase Multifunctional Converter of the Photoelectric System with a Storage Battery for a Local Object with Connection to a Grid. *2020 IEEE Problems of Automated Electrodrive. Theory and Practice (PAEP)*. doi: <https://doi.org/10.1109/paep49887.2020.9240789>
19. Sotnyk, I., Zavdovyeva Y., Zavdovyev, A. (2014). Multi-rate Tariffs in the Management of Electricity Demand. *Mechanism of Economic Regulation*, 2, 106–115. Available at: [https://mer.fem.sumdu.edu.ua/content/acticles/issue\\_21/IRYNA\\_M\\_SOTNYK\\_YULIA\\_N\\_ZAVDOVYEVA\\_ALEXANDER\\_I\\_ZAVDOVYEVMulti\\_Rate\\_Tariffs\\_in\\_the\\_Management\\_of\\_Electricity\\_Demand.pdf](https://mer.fem.sumdu.edu.ua/content/acticles/issue_21/IRYNA_M_SOTNYK_YULIA_N_ZAVDOVYEVA_ALEXANDER_I_ZAVDOVYEVMulti_Rate_Tariffs_in_the_Management_of_Electricity_Demand.pdf)
20. OPzV12-100 (12V100Ah). Hengyang Ritar Power CO.,LTD. Available at: <https://www.ritarpower.com/uploads/ueditor/spec/OPzV12-100.pdf>
21. Shavolkin, O., Shvedchikova, I. (2020). Improvement of the multifunctional converter of the photoelectric system with a storage battery for a local object with connection to a grid. *2020 IEEE KhPI Week on Advanced Technology (KhPIWeek)*. Kharkiv, 287–292.
22. Shavolkin, O., Shvedchikova, I. (2018). Forming of Current of the Single-Phase Grid Inverter of Local Combined Power Supply System with a Photovoltaic Solar Battery. *2018 IEEE 3rd International Conference on Intelligent Energy and Power Systems (IEPS)*. doi: <https://doi.org/10.1109/ieps.2018.8559540>
23. Shavelkin, A., Jasim, J. M. J., Shvedchikova, I. (2019). Improvement of the current control loop of the single-phase multifunctional grid-tied inverter of photovoltaic system. *Eastern-European Journal of Enterprise Technologies*, 6 (5 (102)), 14–22. doi: <https://doi.org/10.15587/1729-4061.2019.185391>
24. Photovoltaic geographical information system. Available at: [https://re.jrc.ec.europa.eu/pvg\\_tools/en/tools.html#SA](https://re.jrc.ec.europa.eu/pvg_tools/en/tools.html#SA)
25. Shavelkin, A., Shvedchikova, I. (2020). Management of generation and redistribution electric power in grid-tied photovoltaic system of local object. *Tekhnichna Elektrodynamika*, 4, 55–59. doi: <https://doi.org/10.15407/techned2020.04.055>